Article

Application of Biosurfactants and Pulsating Electrode Configurations as Potential Enhancers for Electrokinetic Remediation of Petrochemical Contaminated Soil

Brian Gidudu * and **Evans M. Nkhalambayausi Chirwa**

Water Utilisation and Environmental Engineering Division, Department of Chemical Engineering, University of Pretoria, Pretoria 0002, South Africa; evans.chirwa@up.ac.za
* Correspondence: briangid38@gmail.com; Tel.: +27-12-420-5894

Abstract: The remediation of soil contaminated with petrochemicals using conventional methods is very difficult because of the complex emulsions formed by solids, oil, and water. Electrokinetic remediation has of recent shown promising potential in the removal of organics from contaminated media as calls for further improvement of the technology are still made. This work investigated the performance of electrokinetic remediation of soil contaminated with petrochemicals by applying fixed electrode configurations and continuous approaching electrode configurations. This was done in combination with bioremediation by inoculating hydrocarbon degrading bacteria and biosurfactants with the aim of obtaining an improved method of remediation. The results obtained show that the biosurfactant produced by the hydrocarbon degrading bacteria *Pseudomonas aeruginosa* was able to enhance oil extraction to 74.72 ± 2.87%, 57.375 ± 3.75%, and 46.2 ± 4.39% for 185 mm fixed electrodes, 335-260-185 mm continuous approaching electrodes, and 335 mm fixed electrode configurations, respectively. By maintaining high current flow, the 335-260-185 mm continuous approaching electrodes configuration enhanced electroosmotic flow (EOF) on every event of electrodes movement. The fixed electrode configuration of 185 mm provided amiable pH conditions for bacterial growth by allowing quick neutrality of the pH due to high EOF as compared to the 335 mm fixed electrodes configuration. After 240 h, the carbon content in the soil was reduced from 0.428 ± 0.11 mg of carbon/mg of the soil to 0.103 ± 0.005, 0.11355 ± 0.0006, and 0.1309 ± 0.004 for 185 mm, 335-260-185 mm, and 335 mm, respectively. The application of biosurfactants and continuous approaching electrodes reduced the energy expenditure of electrokinetic remediation by enhancing the decontamination process with respect to time.

Keywords: electrokinetic remediation; bioremediation; biosurfactants; electroosmosis; energy

1. Introduction

The petroleum industry has been a great contributor to environmental pollution in the last three decades due to the negative effects it poses to the environment [1]. Petrochemicals are usually composed of petroleum hydrocarbons which are made up of alkanes, cycloalkanes, benzene, toluene, xylenes, phenols, and various polycyclic aromatic hydrocarbons [1]. The greatest concern regarding contamination by these hydrocarbons lies in their mutagenic, carcinogenic, and toxic characteristics [2].

Souza et al. [2] previously argued that hydrocarbons getting into contact with soil may form four different phases. These include the formation of a vapor phase in which the hydrocarbons move to the soil vapor and at times adsorb on the solid surfaces of the soil or dissolve in water. The other is the formation of a free liquid phase which can easily penetrate the soil into the lowest

points reaching groundwater. At times, the hydrocarbons form a dissolved phase if the hydrocarbons are highly hydrophobic forming a hydrocarbon layer on the surface of either the soil or soil water and a plume in groundwater. Lastly, the hydrocarbons can form a residual liquid phase where the hydrocarbons are highly viscous or are adsorbed to the surfaces of the soil particles. The contact of fine solids, oil, and water leads to the formation of stable emulsions which act as a barrier to prevent droplet coalescence because they adsorb at the droplet surface thus lowering the demulsification rate constant [3]. Aliphatics, aromatics, nitrogen sulfur oxygen containing compounds, and asphaltenes are some of the major petrochemical constituents that are preventers of coalescence [4]. Therefore, it is almost impossible to remediate contaminated soil to the satisfactory and admissible levels using conventional remediation technologies [5].

Due to difficulties related to the removal of petrochemical contaminants, numerous methods have been studied and reported regarding remediation of soil contaminated with oil [1]. Considering a variety of improvements made in different remediation methods, some of the methods have now been reported to be effective, but a variety of challenges have still been associated with those methods nevertheless [1]. For example, the use of advanced oxidation processes have been reported to alter soil properties by increasing soil acidity, producing more toxic products, and involving high consumption of energy [6]. Biological treatment methods such as bioremediation, bioattenuation, bioaugmentation, biostimulation, bioventing, and biosparging require long treatment periods to achieve satisfactory decontamination, are inefficient in saline soils, and are only suitable for the treatment of soil contaminated with low molecular weight petroleum hydrocarbons [1]. Chemical treatment methods have issues to do with toxicity and biodegradability of chemicals used to contain, sequester, precipitate, concentrate, separate, and remove contaminants from the polluted soil [7]. Thermal treatment methods are associated with air pollution issues due to exiting flue gases; the treatment alters the chemical, physical and biological properties of the soil, and has high energy requirements [4].

On the other hand, the use of biosurfactants and electrokinetic remediation have captured researchers' attention in recent years. Electrokinetic remediation has the potential to remove volatile organic compounds, BTEX compounds (such as toluene, xylene, benzene, and ethylbenzene), phenols, polychlorinated biphenyls, toluene, chlorophenols, trichloroethane, and total petroleum hydrocarbons from contaminated media even in heterogeneous fine-grained contaminated media where other techniques may not be effective [8]. The decontamination mechanism during electrokinetic remediation involves the movement of the solid phase (colloidal particles) and the liquid phase (oil and water) towards the electrode areas [9]. After the breakdown of colloidal aggregates in the matrix (under the influence of the applied electric field), the colloids move to the oppositely charged electrodes as a result of electrophoresis while the liquid phase (oil and water) moves towards the electrode areas as a result of electroosmosis [9].

For electrokinetic remediation process improvement, researchers have argued that the electrokinetic treatment performance can be improved by the use of solvents, hot water extraction, and surfactants that act as flushing agents to enhance the decontamination mechanisms of electroosmosis, electromigration, and electrophoresis [10,11]. The use of synthetic surfactants is however associated with a range of problems such as environmental toxicity and resistance to biodegradation [12]. Biosurfactants have received increasing attention since they exhibit greater environmental compatibility, more diversity, better surface activity, lower toxicity, higher demulsification ability, higher selectivity, and higher biodegradability [13]. Through micellization, surface tension reduction, increasing contaminant bioavailability to microorganisms, solubilization and increased adsorption, biosurfactants may increase the rate of contaminant removal by altering the surface properties of the matrix leading to the improved motion and coalescence of the contaminants [14]. Biosurfactants can be synthesized by a variety of microorganisms; the production of biosurfactants by a specific isolate can mainly be confirmed if the isolate can exhibit reduction of surface tension below 40 mN/m relative to critical micelle concentration [15].

In electrokinetic remediation, great emphasis is also put on the configuration of the electrodes besides the addition of enhancement additives, consideration of voltage gradient, electrolytes, and operational time because electrode configurations strongly affect the final efficiency of the process and the overall costs [16]. Various electrokinetic improvement interventions have been reported but most have low decontamination efficiencies, lead to extreme increments in treatment costs, and encourage a mass transfer of the contaminants in the remediation process; in fact, the contaminant would still be present in the aqueous phase after treatment [17]. Very few studies have been done regarding the optimization of the electrokinetic process by use of different electrode configuration techniques, combining electrokinetic remediation with other sustainable technologies such as bioremediation and use of biosurfactants [18–20].

To come up with ways of improving the remediation process of petrochemical contaminated media, our study combined the application of biosurfactants, bioremediation, and electrokinetic remediation under pulsating electrode configurations. The study was done by evaluating the performance of the combined process where biosurfactants produced by *Pseudomonas aeruginosa* were applied under different electrode configurations so as to identify strategies that can improve the remediation process either by elimination of the contaminant in the media or separation of the contaminant from the soil. Petrochemical hydrocarbon removal due to variation in pH, bacterial growth, electroosmotic flow, electrophoresis, and electrode configurations was analyzed. The focus was therefore put on the evaluation of the proposed electrode configurations, the effect of biosurfactants, and the effect of combining bioremediation and electrokinetic remediation.

2. Materials and Methods

2.1. Petroleum Contaminated Soils

The properties of the soil used in these experiments are presented in Table 1. The atomic elements in the soil were determined by scanning electron microscopy with energy dispersive spectroscopy (Oxford instruments, Aztec 3.0 SPI software) with an acceleration voltage of 1.5 KV. The soil was sieved using a 2 mm sieve to remove large coarse materials such as leaves and stones and then sterilized at 100 °C in the oven. The soil was then spiked with engine oil obtained from a tribology laboratory at the University of Pretoria to achieve a 150 mL/kg of soil contamination after homogenous mixing using an overhead stirrer and kept for 14 days before experiments. The oil was composed of hexadecane, eicosane, 2,2-dimethyl propane, sulfinyl sulfone, celesticetin, toluene, pentane-1-butoxy, and 2-hexyl-1-octanol.

Table 1. Properties of the soil.

Item No.	Soil Composition	Quantity
1.	Soil type	71% sand, 20% silt, 9% clay
2.	Initial total organic carbon	40 mg/kg
3.	Organic carbon after contamination	428 ± 0.11 mg/kg
4.	Porosity	0.41
5.	Conductivity	274 µS/cm
6.	Particles sizes	74.13% > 425 µm, 21.45%, 425–300 µm, 4.42% < 300 µm
7.	Major elements	O = 48.83 wt%, Al = 3.69 wt%, Si = 26.18 wt%, K = 1.37 wt%, Fe = 7.2 wt%

2.2. Microbial Culture, Media, and Growth Conditions

Strain PA1 (*Pseudomonas aeruginosa*) was obtained from API (atmospheric tank) tank sludge of a refinery in South Africa by selective enrichment to obtain efficient hydrocarbon degraders according to Trummler et al. [21] (Section S1 in Supplementary Materials).

2.3. The Mineral Salt Medium, Screening for Biosurfactant Production, Biosurfactant Production, Recovery, and Purification

The mineral salt medium used in the growth of the strain, the screening, and biosurfactant production methods used are described in detail (Section S1). Biosurfactant production, recovery, and purification was done according to Bezza and Chirwa [22]. The drop collapse method for screening production of biosurfactants was done according to Bodour and Miller-Maier [23], while the oil spreading test was done as described by Morikawa et al. [24].

2.4. Characterization and Identification of Microbial Species

Pure cultures of biosurfactant producing isolates were characterized using the 16S rRNA genotype fingerprinting method. This was achieved by extracting the DNA from the pure cultures according to the protocol described in the Wizard Genomic DNA purification kit (Section S1).

2.5. Biosurfactant Characterization

Characterization of biosurfactants was done by Fourier transform infrared spectroscopy (FTIR), thin layer chromatography (TLC), determination of surface tension, and critical micelle concentration (cmc) according to procedures already reported by other researchers [22] (Section S1).

2.6. Evaluation of Demulsification Capability of the Biosurfactants

Water/oil (W/O) model emulsions of kerosene, hexane or toluene and oil/water (O/W) emulsions of Tween-Triton-kerosene were prepared according to the protocol already reported by other researchers [25] (Section S1) to evaluate the demulsification capability of the biosurfactants.

2.7. Electrokinetic Set Up

The electrokinetic reactor was meticulously constructed from acrylic glass to make three compartments: a soil compartment (160.5 mm × 150 mm × 150 mm) and two electrode compartments (90 mm × 150 mm × 150 mm) so that one of them constituted the anode and the other one the cathode with outlets to electrolyte overflow reservoirs (Figure 1). Distilled water was used as the electrolyte with the electrode-medium compartment interfaces fixed with glass filters (Whatman microfiber Grade GF/A: 1.6 μm) to allow electroosmotic flow across the cell.
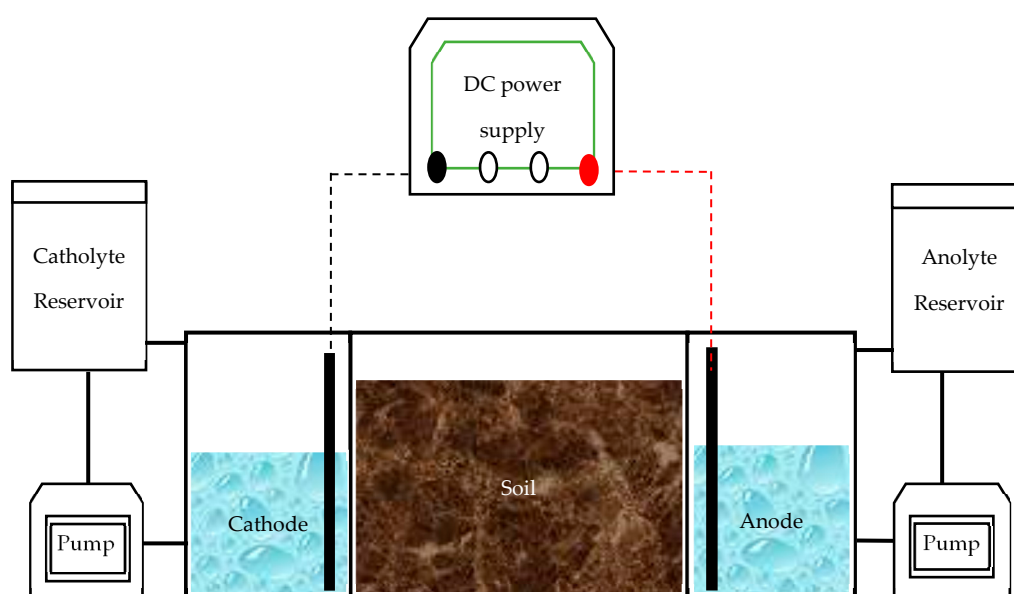

Figure 1. Schematic view of the electrokinetic reactor.

Graphite electrodes (100 mm long × 20 mm diameter) were placed in the electrode compartments at specified distances from each other as a pulsating electrodes configuration. This was to have the anode and cathode fixed electrode spacings of 185 mm and 335 mm as two fixed electrode configurations while the third electrode configuration involved the continuous movement of electrodes after every three days to have continuous electrode spacings of 335 mm, 260 mm, and 185 mm (335-260-185 mm) as a continuous approaching electrode configuration with all the electrodes connected to the DC power supply (0–30 V, 0–3 RS-IPS 303A) of 30 V using stranded iron wires. Experiments with fixed electrode configurations were run for 10 days while in experiments with continuous approaching electrodes, distances were reduced after every three days from 335 mm to 260 mm then to 185 mm. All the experiments had 2 kg of petrochemical contaminated soil inoculated with 30 g of cells resuspended in deionized water (5.43 ± 0.62 log colony forming unit (CFU)/mL) and 26 g/L of biosurfactant supernatant. The control experiment had no biosurfactants or cells and was spiked with 300 mg/L of sodium azide to prevent microbial growth. All experiments were done in triplicate.

The medium compartment was divided into seven sections to the nearest cathode to allow measurements of pH, bacterial growth, and total organic carbon. Electroosmotic flow (EOF), pH, current measurements, and bacterial counts were made after every 24 h. To determine the number of viable cells, 10 mL of an aliquot were picked from each of the seven sections in the soil compartment at 10 mm, 30 mm, 50 mm, 70 mm, 100 mm, 130 mm, and 160 mm horizontal distances from the cathode including samples from the anode and cathode compartments after every 48 h to determine colony forming units (CFUs) at each section as formally described by other researchers [26].

Electroosmotic flow (EOF) in this study was determined as the volume of water or oil (liquid phase) that moved from one compartment to the other. EOF of water was determined as the volume of water that moved from the anode and medium compartments to the cathode compartment while the EOF of oil was determined as the volume of oil that moved from the medium compartment towards the anode compartment. Oil extracted or recovered after the electrokinetic process of remediation was considered as the oil that was displaced from the soil bed to settle on top of the water layer in any of the three reactor compartments. The thickness of the oil on top of the water was measured in each of the compartments and multiplied by the known reactor dimensions (oil thickness/height × length of the compartment × width of the compartment) of the reactor to obtain the volume of oil recovered as was done by other researchers [27]. The oil floating on top of each of the initial constituents of each compartment was referred to as oil extracted because this can be skimmed off by physical means.

2.8. Total Carbon Analysis

Solid samples were picked from each of the seven sections in the soil compartment at 10 mm, 30 mm, 50 mm, 70 mm, 100 mm, 130 mm, and 160 mm horizontal distances from the cathode after 240 h. The samples were air dried for five days and grinded to the smallest particles using a mortar and pestle. The fine samples were ready for analysis in the Schimadzu Total Organic Carbon Analyzer after they were sieved to remain with particles small enough to go through a 600 μm mesh. The solid sample boats were decontaminated of carbon residue by brush washing under flowing tap water followed by rinsing with distilled water. The boats were then soaked in 2 M hydrochloric acid for 10 min and heated in a furnace at 900 °C for 10 min and left to cool before running a sample.

3. Results

3.1. Screening, Isolation, and Identification of the Strain for Hydrocarbon Degradation and Biosurfactant Production

The hydrocarbon degrading and highest biosurfactant producing strain PA1 obtained after isolation and passing of the biosurfactant screening test (using the drop collapse method and the oil spreading test) was identified using the 16S rRNA sequence analysis. The 16S rRNA sequence of PA1

showed the highest similarity to *Pseudomonas aeruginosa* with query cover of 100% as shown in the phylogenetic tree (Figure 2).
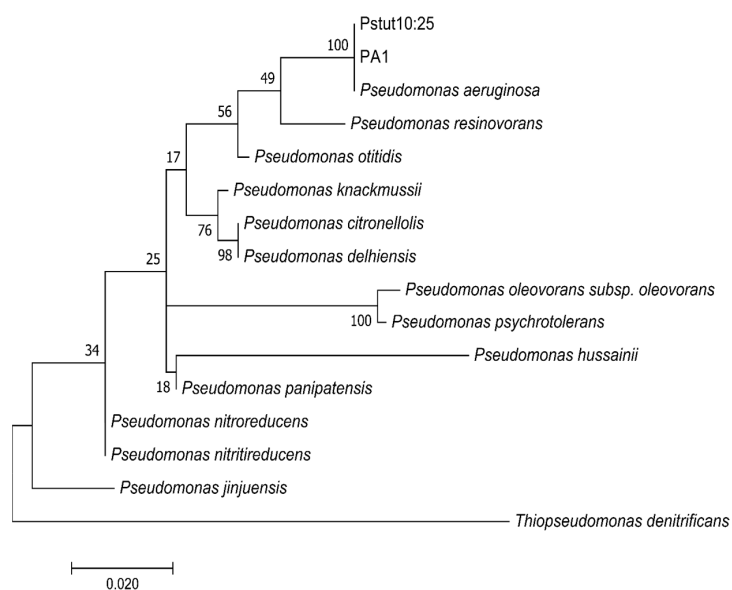

Figure 2. Phylogenetic tree based on the 16S rRNA genotype fingerprinting method with a scale bar corresponding to 0.020 estimated nucleotide distance per sequence position.

3.1.1. Fourier Transform Infrared Spectroscopy (FTIR) Characterization of Biosurfactants

FTIR was used to study the chemical functional groups of the biosurfactants produced by the PA1 strain with fingerprint areas between 4000 cm^{-1} and 400 cm^{-1}. Figure 3 below shows the infrared spectra. The results show a high similarity with typical spectra of glycolipid biosurfactants with the vibrations indicating the presence of rhamnolipids [28,29]. The broad low absorption band at 3336 cm^{-1} represents -OH stretching, peaks at 2920 cm^{-1} and 2849 cm^{-1} reveal stretching vibrations of C-H bands (CH$_2$ and CH$_3$), and the peak at 1737 cm^{-1} shows the presence of C = O. C-H bending is revealed at 1459 cm^{-1} and 899 cm^{-1}, bending of the hydroxyl at 1380 cm^{-1} shows the presence of the carboxylic functional group, while the strong and broad peak at 1153 cm^{-1} and 1118 cm^{-1} is for C-O-C stretching [28].
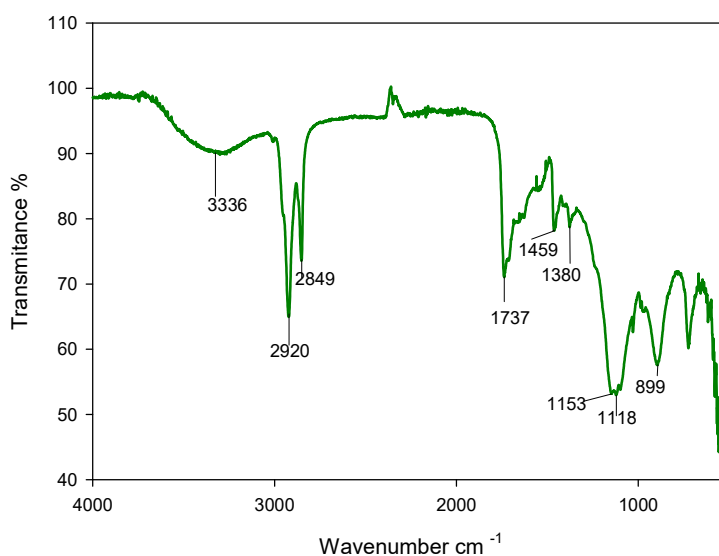

Figure 3. Fourier-transform infrared spectra of the biosurfactant that was produced by the strain PA1.

3.1.2. Thin-Layer Chromatography Analysis

The TLC results of the biosurfactant extracted from the acid precipitate revealed a pink spot on plates with a retardation factor (Rf) value of 0.42 when sprayed with ninhydrin (Figure 4) signifying the presence of amino acids in the biosurfactants similarly reported by other researchers [30]. The low Rf also shows the polar property of the biosurfactant made up of a mono-rhamnolipid [31].
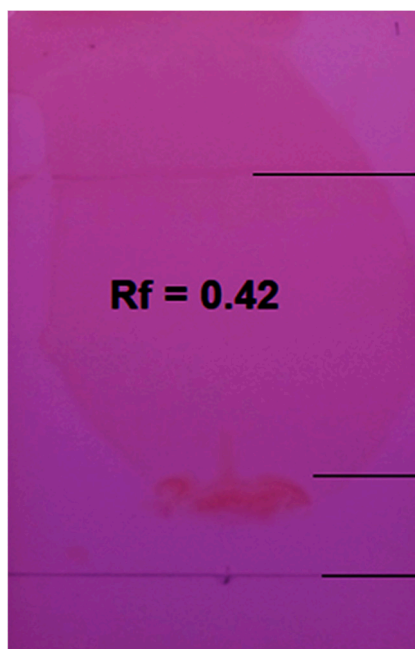

Figure 4. Analysis of thin layer chromatography of the biosurfactant produced by the strain PA1 revealing a pink pigment after spraying with ninhydrin to produce a retardation factor (Rf) of 0.42.

3.1.3. Biosurfactant Yield, Surface Tension, and Critical Micelle Concentration of the Produced Biosurfactant

The yield of biosurfactants during production depends on the culture, carbon source, medium, and environmental conditions [31]. Biosurfactants as surface-active agents are highly dependent on their ability to reduce surface and interfacial tension [30]. The biosurfactants produced reduced the surface tension of water from 71 mN/m to 30.35 mN/m and had a critical micelle concentration value of 156 mg/L relating to results reported by others [32].

3.1.4. Demulsification of Emulsions

The n-hexane W/O emulsion produced the highest demulsification of 85.7% as compared to toluene with 59.3% and kerosene with 55.6% in five days (Section S2, Figures S1 and S2). The O/W emulsion of Tween-Triton-kerosene produced the lowest demulsification of 35.3%. Emulsions with a continuous phase of water were easier to break as compared to those with a continuous phase of kerosene. This can be attributed to the viscosity of the emulsions with emulsions of water being less viscous enabling the breakup of the emulsion as compared to the more viscous emulsions with oil [25]. The findings indicate that the strain produced demulsifiers with the ability to easily break emulsions with only one type of organic phase as compared to those with multiple organic phases which is in agreement with some previous reports [25,33]. The ability of the surface-active agent produced by *Pseudomonas aeruginosa* strain PA1 to break emulsions shows that the surface-active agent produced is a biosurfactant with the ability to emulsify immiscible liquids and demulsify or break emulsions as compared to bioemulsifiers that only have the capacity to emulsify [34].

3.2. Bio-Electrokinetic Remediation

3.2.1. Variation of Current during Bio-Electrokinetic Treatment

Figure 5 shows the variation of current for the entire process of electrokinetic remediation. Since a constant voltage of 30 V was applied throughout the experiments the results demonstrate the effect of resistance on current flow because of decreased conductivity. The current flow in the system was majorly low because of the low voltage of 30 V that was applied. The highest current in the fixed electrode configurations was 2.306 ± 0.095 mA for 185 mm and 2.305 ± 0.005 for 335 mm. The 335-260-185 mm continuous approaching electrode configuration had 2.3 ± 0.02 mA as the highest current. Much as a constant voltage was applied, there were some minor differences noticed in the current with different electrode configurations. This is because of the differences in electrode configurations where the current in the fixed 335 mm electrode configuration continuously drops because of an increase in resistance. The high resistance in the fixed 335 mm electrode configuration is due to the long distance between electrodes relative to Ohm's law. The current in the 185 mm fixed electrode configuration remains slightly higher than that of the fixed 335 mm electrode configuration after 100 h because of the shorter distances between electrodes. In the 335-260-185 mm continuous approaching electrode configuration, the current flow is generally maintained high as compared to the fixed electrode configurations because on every movement of the electrodes towards each other, the resistance in the system is reduced according to Ohm's law. The overlapping error bars in Figure 5 are due to the changes brought about by the minor differences in the quantity of ionic species in the soil for every individual experiment.
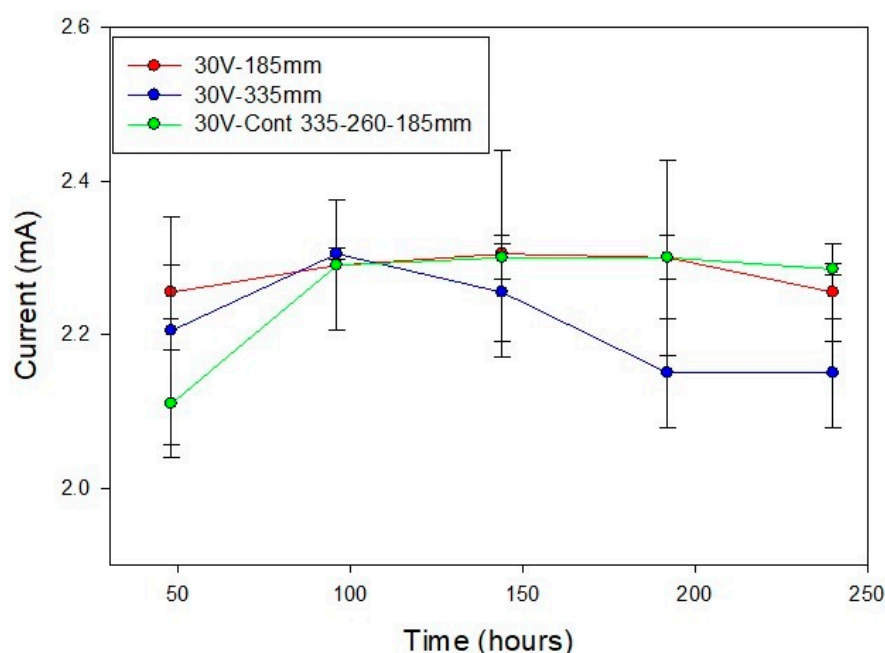

Figure 5. Variation of current for fixed electrode configurations of 185 mm and 335 mm and the continuous approaching electrode configuration of 335-260-185 mm. Data are expressed as mean ± standard deviation of three replicates.

To improve electrokinetic remediation, resistance must be decreased to enhance electromigration, electro-coalescence, and electroosmosis which aid in improving the removal of contaminants from the contaminated media [35]. In all the experiments, the current starts low then gradually increases due to disassociation of water producing OH^- ions at the cathode and H^+ ions at the anode which, besides the other ionic species in the soil, increase the ionic strength of the system leading to an increase in the current [36]. Then the current starts reducing in all experiments especially after 200 h not only due to

resistance in the interface between electrodes but also because ions with positive or negative charges move to the two ends of the electrokinetic cell as a consequence of electromigration.

The result is the drop of ionic strength in the soil leading to a decrease in the current [8]. Comparing current flow in all experiments it was evident that the 185 mm fixed electrode configuration enhanced current flow for longer hours as compared to the 335 mm fixed electrode configuration, but the 335-260-185 mm continuous approaching electrode configuration maintained higher current flow than in experiments with fixed electrode configurations.

3.2.2. Variation of Electroosmotic Flow of Water during Bio-Electrokinetic Treatment

To achieve efficient electrokinetic removal of contaminants, the processes of EOF, electromigration, and electrophoresis must be improved [37,38]. When an electric field is applied it leads to the movement of the liquid phase (water and oil) due to the existence of the electrical double layer at the interface of the water/oil and the solid surface, but also due to the migration of charged particles or ions in a colloidal system towards the counter charged electrode [36]. Electroosmosis is affected by various factors including current, viscosity, ionic concentration, temperature, the dielectric constant of the interstitial fluid, and surface charge of the solid matrix, among others [36]. According to the Helmholz–Smoluchowski theory, current is directly proportional to EOF. Figure 6 demonstrates this relationship where the 185 mm fixed electrode configuration had higher EOF as compared to the 335 mm fixed electrode configuration. The average highest EOF in volumetric terms for all experiments was 2.0225×10^{-4} m^3, 1.64×10^{-4} m^3, and 1.62×10^{-4} m^3 for 185 mm, 335-260-185 mm, and 335 mm, respectively. This shows a direct relationship between EOF and current if the two parameters are to be compared.
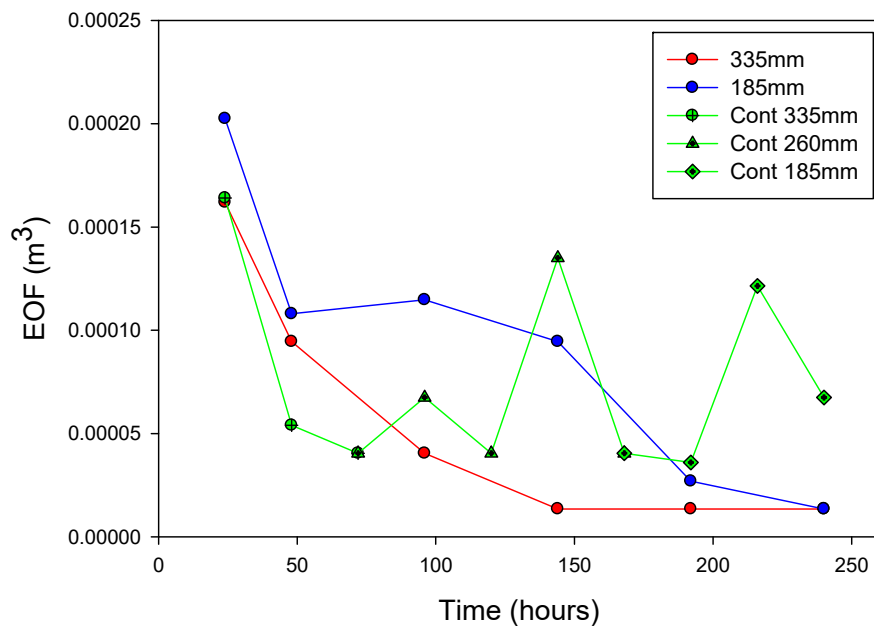

Figure 6. Time course of electroosmotic flow (EOF) of water for fixed electrode configurations of 185 mm and 335 mm and the continuous approaching electrode configuration of 335-260-185 mm. Data are expressed as the mean of three replicates.

In all experiments, EOF started high but in the 335 mm fixed electrode configuration, there was a gradual reduction in EOF just like it was observed with the current. After 100 h, EOF was also seen to gradually reduce up to the end of the experiment in the 185 mm fixed electrode configuration. In the 335-260-185 mm continuous approaching electrode configuration, EOF increased after every reduction in the distances between electrodes. The same was also reported by Li et al. [39], whereby a different approaching electrode strategy from the one used here had been employed. The increase

in current on every event of approaching electrodes or reduction in the distance between electrodes (from 335 mm to 260 mm to 185 mm) is due to a reduction in the electrolytic distance between the working electrodes. The new short electrolytic distance obtained after every movement increases H^+ ions and high redox potential concentrations which quickly migrate to the cathode. This is because a new shorter distance to be traveled by the low strength ions in the pore fluid is created leading to a reduction in the resistance of the matrix or reactions between the migrating ions and the matrix species [15]. In all experiments, the EOF of water was observed to be towards the cathode from the anode because of the negatively charged surface of the soil [35].

3.2.3. Oil Extraction from the Contaminated Soil during Bio-Electrokinetic Treatment

Oil extraction from the contaminated soil was observed in all the experiments. Since EOF drives the liquid phase from one compartment to another due to the existence of the electrical double layer at the interface of the water/oil and the solid surface, EOF of oil was also observed. Oil extraction started with the vertical displacement of the oil from the soil bed to the top of the soil followed by the horizontal electroosmotic flow from the medium compartment to the electrode compartments. In the presence of biosurfactants, the oil removal from soil was 74.72 ± 2.87%, 57.375 ± 3.75%, and 46.2 ± 4.39% for 185 mm, 335-260-185 mm, and 335 mm electrode configurations, respectively (Figure 7a). The highest oil extraction was observed between the start of the experiment to 100 h.
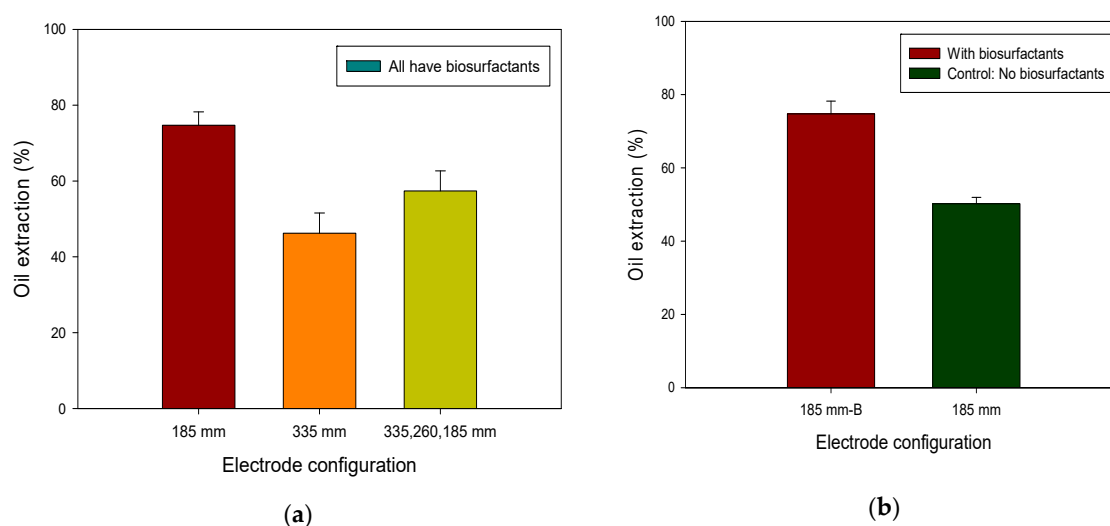

Figure 7. (**a**) Oil extraction in the presence of biosurfactants; (**b**) oil extraction in the presence and absence of biosurfactants. Data are expressed as mean ± standard deviation of three replicates.

To determine the effect of biosurfactants in the remediation process, the 185 mm fixed electrode configuration with biosurfactants was compared to the experiments run in the absence of biosurfactants (Figure 7b). The results show that the experiments that had biosurfactants, high current flow, and enhanced EOF flow had the highest oil extraction. Figure 7b demonstrates that biosurfactants improve the removal process of petrochemicals as compared to when they are not used. This is because of the combined effect of demulsification due to application of biosurfactants, and electro-demulsification and electro-coalescence that are as a result of the application of the electric field. Biosurfactants enhance demulsification by adsorbing to oil/water interfaces where they react with the existing emulsifiers, such as asphaltenes and resins, resulting in the elimination of the thin film at the oil and water interfaces [17]. This promotes the coalescence of the dispersed droplets leading to three distinct continuous phases of solids, oil, and water that can then be moved by EOF from the medium compartment to any electrode compartment [40]. The EOF flow of oil was mainly seen from the medium compartment towards the anode compartment opposite to the EOF of water. This was because of the competition between water molecules and oil molecules at the cathode-medium compartment.

In the presence of this liquid phase competition, the smaller molecules of water outcompete the oil molecules. This leads to the movement of oil to the anode which was opposite to the direction of EOF of water.

3.2.4. Variation in pH and Its Effect on Bacterial Growth during the Bio-Electrokinetic Treatment

When an electric field is applied during electrokinetic treatment, decomposition of water occurs at the electrodes [36]. Oxidation reactions occur at the anode and reduction reactions occur at the cathode as seen in Equations (1) and (2), respectively [41,42].

$$2H_2O \rightarrow 4e^- + 4H^+_{(aq)} + O_{2(g)} \tag{1}$$

$$4H_2O + 4e^- \rightarrow 2H_{2(g)} + 4OH^-_{(aq)} \tag{2}$$
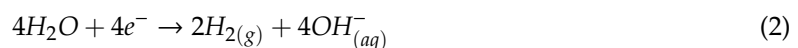
These reactions lead to the formation of the alkaline front at the cathode and an acid front at the anode on the immediate application on an electric field; but as ions start migrating, the pH dynamically changes across the system as the H^+ ions move towards the cathode [41]. With H^+ almost twice mobile (1.75 times) as OH^-, the protons dominate resulting in the movement of the acid front towards the cathode where H^+ ions meet OH^- ions and form water [42]. The pH in the system is, therefore, dependent on the movement of H^+ and OH^- across the system [36,42]. To determine the variation of pH and its effect on bacterial growth, due to the application of different electrode configuration strategizes, the fixed electrode configurations of 185 mm and 335 mm were used for analysis. These extremes also demonstrated what probably happens with the continuous approaching electrode configurations.

On average, the highest pH was noticed at the areas near the cathode and the lowest pH was noticed at areas near the anode (Figure 8). Within the medium compartment where the soil is accommodated, the average pH ranged between 10.13 and 5.43 for 185 mm while the pH ranged between 7.16 and 3.09 for 335 mm. In general, the pH would rise from 7 to as high as 12.7 in the cathode compartment due to reduction reactions while in the anode compartment pH would decrease to as low as 2.2 due to oxidation reactions. Comparing the variation of pH between 185 mm and 335 mm it is noticed that the 185 mm fixed electrode configuration imposed high pH in the system as compared to the 335 mm fixed electrode configuration, where highly acidic conditions were observed (Figure 8).
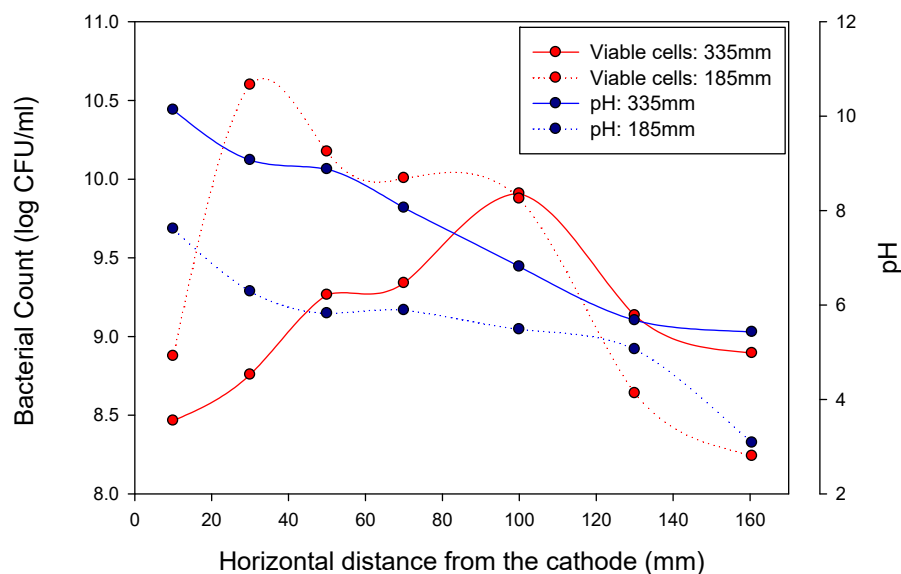

Figure 8. Variation of pH and bacterial growth for fixed electrode configurations. Data are expressed as mean of three replicates.

Microbial growth was determined using viable cell counts in different sections of the reactor to determine the effect of different electrode configurations on microbial growth. Figure 8 shows that the areas between 40 mm and 120 mm horizontal distance from the cathode supported the highest bacterial growth. The region between 40 mm and 120 mm horizontal distance from the cathode was the region that was furthest from the extremely alkaline conditions near the cathode and extremely acidic conditions near the anode. The pH in this region predominantly presented amiable pH conditions that supported bacterial growth. This is scientifically agreeable because previous studies have shown that bacteria can grow under a wide range of pH but the optimum pH conditions for *Pseudomonas aeruginosa* are pH 7 [43].

Comparing the two fixed electrode configurations, an average viable cell count between 9.9082 and 8.4657 log CFU/mL was determined for the 335 mm while cell counts between 10.56 and 8.2 log CFU/mL were determined for the 185 mm electrode configuration. Although not too extensive, the differences in the microbial counts are because the 185 mm fixed electrode configuration offered a more amiable pH environment for microbial growth as compared to the 335 mm fixed electrode configuration.

The pH in the medium compartment for the 185 mm fixed electrode configuration was closer to the optimum pH condition of 7 as compared to the 335 mm electrode configuration. Viable cell counts showed that bacteria were present in all reactor compartments due to electroosmosis and electrophoresis that are mainly used as the transport mechanisms of the bacteria [18]. As much as bacterial growth was substantially affected by the vacillating pH, the transport mechanisms of electroosmosis and electrophoresis still move bacteria to all sections of the reactor.

3.2.5. Effect of Electrode Configuration and Application of Biosurfactants on Hydrocarbon Removal

The removal of contaminants from contaminated media mainly relies on EOF and electrophoresis [16]. In this study, the results in Figure 9a show that the fixed electrode configuration of 185 mm had the highest carbon removal followed by the 335-260-185 mm continuous approaching electrode configuration. EOF, current, oil extraction, pH, and bacterial growth variations have already been discussed in detail. The results obtained here demonstrate that the experiments that predominantly maintained the highest current flow, EOF, oil extraction, and supported the most stable bacterial growth had the highest carbon removal. Carbon content was reduced from 0.428 ± 0.11 mg of carbon/mg of the soil to 0.103 ± 0.005 for 185 mm, 0.11355 ± 0.0006 for 335-260-185 mm, and 0.1309 ± 0.004 for 335 mm. The highest carbon removal was therefore observed in the 185 mm fixed electrode configuration while the lowest carbon removal was observed in 335 mm fixed electrode configuration.
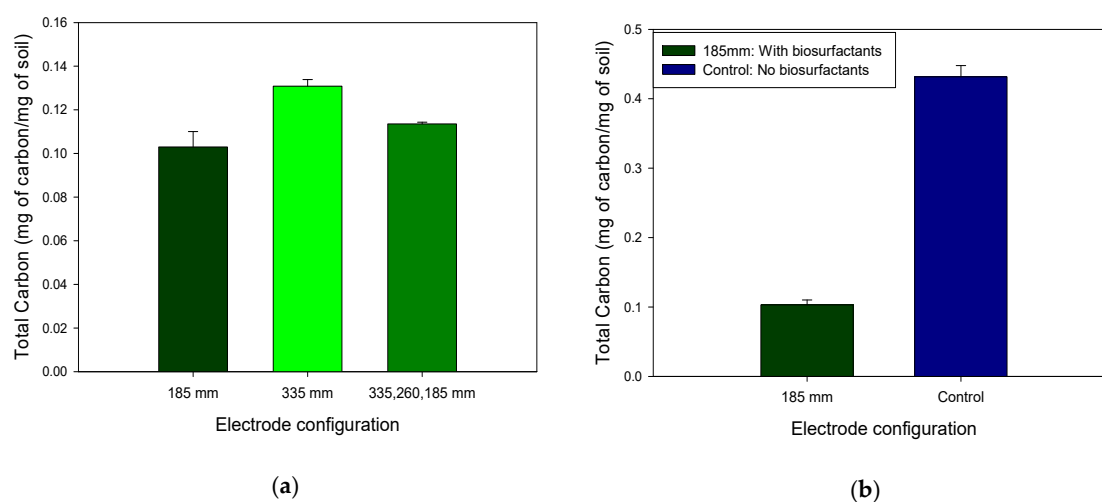

(a) (b)

Figure 9. (**a**) Total carbon remaining in the soil in the presence of biosurfactants after bio-electrokinetic remediation; (**b**) total carbon remaining in the soil after electrokinetic remediation in the presence and absence of biosurfactants. Data are expressed as mean ± standard deviation of three replicates.

To determine the effect of biosurfactants on the hydrocarbon removal, Figure 9b shows that the experiment that was operated without biosurfactants or cells had a lower removal of petrochemical hydrocarbons (0.266 ± 0.014 mg of carbon/mg of the soil) as compared to the experiments where biosurfactants were applied (0.103 ± 0.005 mg of carbon/mg of the soil). The effect of the biosurfactants on petrochemical hydrocarbon extraction has been discussed in detail in Section 3.2.3. By improving demulsification and coalescence, biosurfactants enhance the removal of the contaminants from the contaminated media. Biosurfactants also improve the bioavailability of the recalcitrant hydrocarbons to the microbes thereby increasing the degradation of the contaminants [14].

The remediation of contaminated media such as soil in this study by use of electrokinetic remediation majorly relies on the removal of the contaminant by moving it from the soil (medium compartment) to the other compartments if available [40]. This may not necessarily lead to the elimination of the contaminant since the contaminant is simply moved from the soil to another compartment. By combining electrokinetic remediation and bioremediation, petrochemicals could be recovered in the anode compartment for purposes of reuse, but the remaining hydrocarbons in the soil were degraded by the hydrocarbon degrading bacteria to have total elimination of the contaminant. Figure 8 in Section 3.2.4 has already shown that bacterial growth was substantially affected by pH in different regions of the soil. This also led to non-linearity in the degradation of the contaminants in the soil with regions between 40 mm and 120 mm horizontal distance from the cathode having the lowest total carbon content after the bio-electrokinetic remediation process.

3.2.6. Effect of Electrode Configuration and Application of Biosurfactants on Energy Expenditure

Energy expenditure was calculated according to Equation (3), where V_s is the volume of the medium (soil), V is the voltage difference between the electrodes, and I is the electric current. E_u is therefore calculated as kWh m^{-3}.

$$E_u = \frac{1}{V_S} \int VI dt \qquad (3)$$

Although the differences in energy expenditure were not substantial, in the presence of biosurfactants, the energy expenditure was highest in the 185 mm fixed electrode configuration while the lowest energy expenditure was in the 335 mm fixed electrode configuration. The energy expenditure was determined as 8.52 ± 0.4293, 8.42 ± 0.2285, and 8.1084 ± 0.0104 kWh m^{-3} for 185 mm, 335-260-185 mm, and 335 mm respectively (Figure 10a). The 185 mm fixed electrode configurations with and without biosurfactants were compared in Figure 10b to determine the effect of biosurfactants on energy expenditure. The energy expenditure in the 185 mm fixed electrode configuration with biosurfactants (8.52 ± 0.4293 kWh m^{-3}) was lower than when biosurfactants were not applied (8.825 ± 0.015 kWh m^{-3}). The results show that for satisfactory remediation to be achieved while reducing the energy, electrokinetic remediation had to be combined with biosurfactants. Biosurfactants improve demulsification which enhances EOF of the hydrocarbon contaminants from the soil in combination with electro-demulsification and electro-coalescence. The combination of these three inputs leads to energy saving as compared to when electrokinetic remediation is done in the absence of biosurfactants. It was also observed that so long as a constant voltage is applied, the differences in current and energy expenditure are low.

The results have also shown that satisfactory remediation is efficiently achieved by the 185 mm fixed electrode configuration (Figure 9). The 185 mm fixed electrode configuration requires low electrode spacing which leads to an increase in general treatment costs in terms of electrode requirements and energy expenditure. Applying an electrode configuration with a low electrode spacing means more electrodes would be needed in onsite remediation hence increasing the remediation cost. The approaching electrode configuration, on the other hand, seems to have moderate removal of the contaminants at a lower energy cost, which if combined with bioremediation, makes the process more cost-effective. This is because after 240 h, for example, 57.375 ± 3.75% of the oil was removed from the soil, and the remaining oil in the soil media can then be utilized as a carbon source by the microbes to

have total elimination of the petrochemical contaminant from the soil. This is important considering that bioremediation has been reported to require long time treatment periods to achieve satisfactory decontamination [1]. Therefore, the use of 335-260-185 mm continuous approaching electrode would offer satisfactory decontamination with reduced time requirements and reduced energy expenditure.
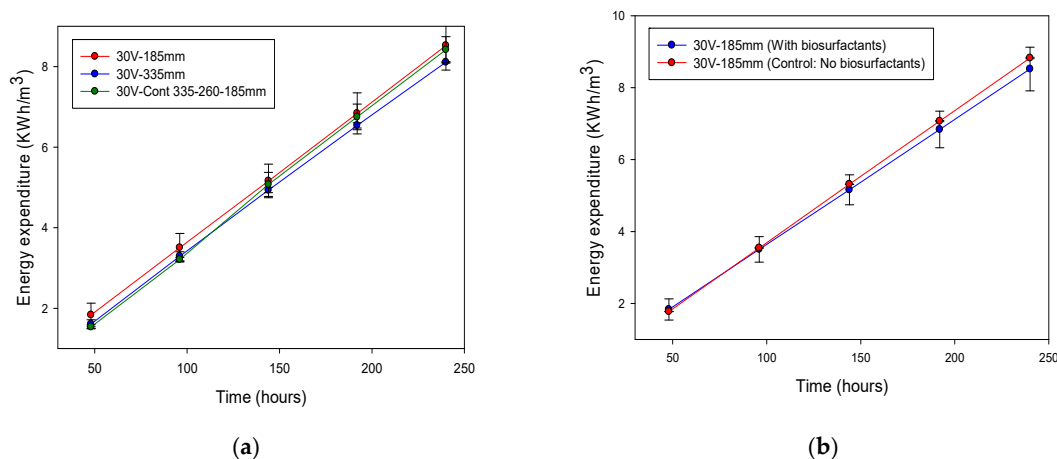

| (a) | (b) |

Figure 10. (**a**) Energy expenditure in the presence of biosurfactants during bio-electrokinetic remediation; (**b**) energy expenditure in the presence and absence of biosurfactants. Data are expressed as mean ± standard deviation of three replicates.

4. Conclusions

The rhamnolipid biosurfactant produced by the hydrocarbon-degrading bacteria *Pseudomonas aeruginosa* affected the desorption of the petrochemical contaminants from the contaminated soil. The enhancement of desorption improved the coalescence of the contaminants which led to an enhanced electroosmotic flow of the petrochemical pollutants from the soil. This was shown by the oil extraction efficiencies of 74.72 ± 2.87%, 57.375 ± 3.75%, and 46.2 ± 4.39% for 185 mm fixed electrodes, 335-260-185 mm continuous approaching electrodes, and 335 mm fixed electrode configurations, respectively. The 335-260-185 mm continuous approaching electrode configuration maintained high current flow and electroosmotic flow in the system on every event of electrode movement which was absent in fixed electrode configurations.

The 185 mm fixed electrode configuration provided amiable pH conditions for bacterial growth as compared to the 335 mm fixed electrode configuration. By supporting bacterial growth, the reactor simultaneously removed the petrochemical contaminants by bioremediation and electrokinetic remediation. In the presence of bioremediation, electrokinetic remediation was not only a remediation technology that removed a contaminant from soil to another phase but also led to the total elimination of the contaminant from the soil by microbial degradation. The combination of electrokinetic remediation, bioremediation, and application of biosurfactants was able to achieve satisfactory decontamination especially with the 185 mm fixed electrode configuration by reducing the carbon content of soil from 0.428 ± 0.11 mg of carbon/mg of the soil to 0.103 ± 0.005, 0.11355 ± 0.0006, 0.1309 ± 0.004 for 185 mm, 335-260-185 mm and 335 mm, respectively. The energy expenditure was however highest when the 185 mm fixed electrode configuration was used. Application of a higher voltage and use of 2D electrode configurations are proposed for further field-scale studies in naturally occurring complex geochemistry where highly reactive ions on the soil surface would be present to confirm these results.

References

1. Ossai, I.C.; Ahmed, A.; Hassan, A.; Hamid, F.S. Remediation of soil and water contaminated with petroleum hydrocarbon: A review. *Environ. Technol. Innov.* **2020**, *17*. [CrossRef]

2. Souza, E.C.; Vessoni-Penna, T.C.; de Souza Oliveira, R.P. Biosurfactant-enhanced hydrocarbon bioremediation: An overview. *Int. Biodeter. Biodegr.* **2014**, *89*, 88–94. [CrossRef]

3. Elektorowicz, M.; Habibi, S.; Chifrina, R. Effect of electrical potential on the electro-demulsification of oily sludge. *J. Colloid Interface Sci.* **2006**, *295*, 535–541. [CrossRef] [PubMed]

4. Hu, G.; Li, J.; Zeng, G. Recent development in the treatment of oily sludge from petroleum industry: A review. *J. Hazard. Mater.* **2013**, *261*, 470–490. [CrossRef] [PubMed]

5. Yeung, A.T.; Gu, Y.Y. A review on techniques to enhance electrochemical remediation of contaminated soils. *J. Hazard. Mater.* **2011**, *195*, 11–29. [CrossRef]

6. Zhang, T.; Liu, Y.; Zhong, S.; Zhang, L. AOPs-based remediation of petroleum hydrocarbons-contaminated soils: Efficiency, influencing factors and environmental impacts. *Chemosphere* **2019**, *246*, 125726. [CrossRef]

7. Karthick, A.; Roy, B.; Chattopadhyay, P. A review on the application of chemical surfactant and surfactant foam for remediation of petroleum oil contaminated soil. *J. Environ. Manag.* **2019**, *243*, 187–205. [CrossRef]

8. Ammami, M.T.; Portet-Koltalo, F.; Benamar, A.; Duclairoir-Poc, C.; Wang, H.; Le Derf, F. Application of biosurfactants and periodic voltage gradient for enhanced electrokinetic remediation of metals and PAHs in dredged marine sediments. *Chemosphere* **2015**, *125*, 1–8. [CrossRef]

9. Kim, B.-K.; Baek, K.; Ko, S.-H.; Yang, J.-W. Research, and field experiences on electrokinetic remediation in South Korea. *Sep. Purif. Technol.* **2011**, *79*, 116–123. [CrossRef]

10. Electorowicz, M.; Hatim, J. Application of surfactant enhanced electrokinetics for hydrocarbon contaminated soils. Paper presented at the 53rd Canadian Geotechnical Conference, Montreal, QC, Canada, 15–18 October 2000; pp. 617–624.

11. Boulakradeche, M.O.; Akretche, D.E.; Cameselle, C.; Hamidi, N. Enhanced electrokinetic remediation of hydrophobic organics contaminated soils by the combination of non-ionic and ionic surfactants. *Electrochim. Acta* **2015**, *174*, 1057–1066. [CrossRef]

12. Mulligan, C.N.; Yong, R.N.; Gibbs, B.F. Surfactant-enhanced remediation of contaminated soil: A review. *Eng. Geol.* **2001**, *60*, 371–380. [CrossRef]

13. Sun, S.; Wang, Y.; Zang, T.; Wei, J.; Wu, H.; Wei, C.; Li, F. A biosurfactant-producing Pseudomonas aeruginosa S5 isolated from coking wastewater and its application for bioremediation of polycyclic aromatic hydrocarbons. *Bioresour. Technol.* **2019**, *281*, 421–428. [CrossRef] [PubMed]

14. Batista, S.B.; Mounteer, A.H.; Amorim, F.R.; Totola, M.R. Isolation and characterization of biosurfactant/bioemulsifier-producing bacteria from petroleum contaminated sites. *Bioresour. Technol.* **2006**, *97*, 868–875. [CrossRef] [PubMed]

15. Tang, J.; He, J.; Liu, T.; Xin, X.; Hu, H. Removal of heavy metal from sludge by the combined application of a biodegradable biosurfactant and complexing agent in enhanced electrokinetic treatment. *Chemosphere* **2017**, *189*, 599–608. [CrossRef]

16. Kim, W.S.; Jeon, E.K.; Jung, J.M.; Jung, H.B.; Ko, S.H.; Seo, C.I.; Baek, K. Field application of electrokinetic remediation for multi-metal contaminated paddy soil using two-dimensional electrode configuration. *Environ. Sci. Pollut. Res. Int.* **2014**, *21*, 4482–4491. [CrossRef] [PubMed]

17. Pourfadakari, S.; Ahmadi, M.; Jaafarzadeh, N.; Takdastan, A.; Neisi, A.A.; Ghafari, S.; Jorfi, S. Remediation of PAHs contaminated soil using a sequence of soil washing with biosurfactant produced by Pseudomonas aeruginosa strain PF2 and electrokinetic oxidation of desorbed solution, effect of electrode modification with Fe_3O_4 nanoparticles. *J. Hazard. Mater.* **2019**, *379*, 120839. [CrossRef] [PubMed]

18. Mena, E.; Villaseñor, J.; Rodrigo, M.A.; Cañizares, P. Electrokinetic remediation of soil polluted with insoluble organics using biological permeable reactive barriers: Effect of periodic polarity reversal and voltage gradient. *Chem. Eng. J.* **2016**, *299*, 30–36. [CrossRef]

19. Tang, J.; He, J.; Xin, X.; Hu, H.; Liu, T. Biosurfactants enhanced heavy metals removal from sludge in the electrokinetic treatment. *Chem. Eng.* **2018**, *334*, 2579–2592. [CrossRef]

20. Alshawabkeh, A.N. Electrokinetic Soil Remediation: Challenges and Opportunities. *Sep. Sci. Technol.* **2009**, *44*, 2171–2187. [CrossRef]

21. Trummler, K.; Effenberger, F.; Syldatk, C. An integrated microbial/enzymatic process for production of rhamnolipids and L-(+)-rhamnose from rapeseed oil with Pseudomonas sp. DSM 2874. *Eur. J. Lipid Sci. Technol.* **2003**, *105*, 563–571. [CrossRef]

22. Bezza, F.A.; Chirwa, E.M.N. Biosurfactant from Paenibacillus dendritiformis and its application in assisting polycyclic aromatic hydrocarbon (PAH) and motor oil sludge removal from contaminated soil and sand media. *Process. Saf. Environ.* **2015**, *98*, 354–364. [CrossRef]

23. Bodour, A.A.; Miller-Maier, R.M. Application of a modified drop-collapse technique for surfactant quantitation and screening of biosurfactant-producing microorganisms. *J. Microbiol. Methods* **1998**, *32*, 273–280. [CrossRef]

24. Morikawa, M.; Hirata, Y.; Imanaka, T. A study on the structure–function relationship of lipopeptide biosurfactants. *Biochim. Biophys. Acta* **2000**, *1488*, 211–218. [CrossRef]

25. Coutinho, J.O.; Silva, M.P.; Moraes, P.M.; Monteiro, A.S.; Barcelos, J.C.; Siqueira, E.P.; Santos, V.L. Demulsifying properties of extracellular products and cells of Pseudomonas aeruginosa MSJ isolated from petroleum-contaminated soil. *Bioresour. Technol.* **2013**, *128*, 646–654. [CrossRef] [PubMed]

26. APHA. Standard methods for the examination of water and wastewater. In *Water Environment Federation*, 25th ed.; Eaton, A.D., Clesceri, L.S., Rice, E.W., Greenberg, A.E., Franson, M.A.H., Eds.; American Public Health Association: Washington, DC, USA, 2005.

27. Dastgheib, S.M.; Amoozegar, M.A.; Elahi, E.; Asad, S.; Banat, I.M. Bioemulsifier production by a halothermophilic Bacillus strain with potential applications in microbially enhanced oil recovery. *Biotechnol. Lett.* **2008**, *30*, 263–270. [CrossRef] [PubMed]

28. Fadhile Almansoory, A.; Abu Hasan, H.; Idris, M.; Sheikh Abdullah, S.R.; Anuar, N.; Musa Tibin, E.M. Biosurfactant production by the hydrocarbon-degrading bacteria (HDB) Serratia marcescens: Optimization using central composite design (CCD). *J. Ind. Eng. Chem.* **2017**, *47*, 272–280. [CrossRef]

29. Rikalovic, M.; Gojgic-Cvijovic, G.; Vrvic, M.; Karadzic, I. Production, and characterization of rhamnolipids from Pseudomonas aeruginosa san ai. *J. Serb. Chem. Soc.* **2012**, *77*, 27–42. [CrossRef]

30. Sriram, M.I.; Gayathiri, S.; Gnanaselvi, U.; Jenifer, P.S.; Mohan Raj, S.; Gurunathan, S. Novel lipopeptide biosurfactant produced by hydrocarbon degrading and heavy metal tolerant bacterium Escherichia fergusonii KLU01 as a potential tool for bioremediation. *Bioresour. Technol.* **2011**, *102*, 9291–9295. [CrossRef]

31. George, S.; Jayachandran, K. Production and characterization of rhamnolipid biosurfactant from waste frying coconut oil using a novel Pseudomonas aeruginosa D. *J. Appl. Microbiol.* **2013**, *114*, 373–383. [CrossRef] [PubMed]

32. Câmara, J.M.D.A.; Sousa, M.A.S.B.; Barros Neto, E.L.; Oliveira, M.C.A. Application of rhamnolipid biosurfactant produced by Pseudomonas aeruginosa in microbial-enhanced oil recovery (MEOR). *J. Petrol. Explor. Prod. Tech.* **2019**. [CrossRef]

33. Huang, X.F.; Liu, J.; Lu, L.J.; Wen, Y.; Xu, J.C.; Yang, D.H.; Zhou, Q. Evaluation of screening methods for demulsifying bacteria and characterization of lipopeptide bio-demulsifier produced by Alcaligenes sp. *Bioresour. Technol.* **2009**, *100*, 1358–1365. [CrossRef] [PubMed]

34. Uzoigwe, C.; Burgess, J.G.; Ennis, C.J.; Rahman, P.K. Bioemulsifiers are not biosurfactants and require different screening approaches. *Front. Microbiol.* **2015**, *6*, 245. [CrossRef] [PubMed]

35. Yang, L.; Nakhla, G.; Bassi, A. Electro-kinetic dewatering of oily sludges. *J. Hazard. Mater.* **2005**, *125*, 130–140. [CrossRef] [PubMed]

36. Cameselle, C.; Gouveia, S.; Akretche, D.E.; Belhadj, B. Advances in Electrokinetic Remediation for the Removal of Organic Contaminants in Soils. 2013. Available online: http://www.intechopen.com/books/organic-pollutants-monitoringrisk-and-treatment (accessed on 20 June 2020).

37. Rozas, F.; Castellote, M. Electrokinetic remediation of dredged sediments polluted with heavy metals with different enhancing electrolytes. *Electrochim. Acta* **2012**, *86*, 102–109. [CrossRef]

38. Agnew, K.; Cundy, A.B.; Hopkinson, L.; Croudace, I.W.; Warwick, P.E.; Purdie, P. Electrokinetic remediation of plutonium-contaminated nuclear site wastes: Results from a pilot-scale on-site trial. *J. Hazard. Mater.* **2011**, *186*, 1405–1414. [CrossRef] [PubMed]

39. Li, G.; Guo, S.; Li, S.; Zhang, L.; Wang, S. Comparison of approaching and fixed anodes for avoiding the 'focusing' effect during electrokinetic remediation of chromium-contaminated soil. *Chem. Eng.* **2012**, *203*, 231–238. [CrossRef]

40. Rocha, E.S.F.C.P.; Roque, B.A.C.; Rocha, E.S.N.M.P.; Rufino, R.D.; Luna, J.M.; Santos, V.A.; Banat, I.M.; Sarubbo, L.A. Yeasts and bacterial biosurfactants as demulsifiers for petroleum derivative in seawater emulsions. *AMB Express* **2017**, *7*, 202. [CrossRef] [PubMed]

41. Jeon, E.K.; Jung, J.M.; Kim, W.S.; Ko, S.H.; Baek, K. In situ electrokinetic remediation of As-, Cu-, and Pb-contaminated paddy soil using hexagonal electrode configuration: A full-scale study. *Environ. Sci. Pollut. Res. Int.* **2015**, *22*, 711–720. [CrossRef] [PubMed]

42. Shu, J.; Liu, R.; Liu, Z.; Du, J.; Tao, C. Electrokinetic remediation of manganese and ammonia nitrogen from electrolytic manganese residue. *Environ. Sci. Pollut. Res. Int.* **2015**, *22*, 16004–16013. [CrossRef]

43. Das, K.; Mukherjee, A.K. Crude petroleum-oil biodegradation efficiency of Bacillus subtilis and Pseudomonas aeruginosa strains isolated from a petroleum-oil contaminated soil from North-East India. *Bioresour. Technol.* **2007**, *98*, 1339–1345. [CrossRef] [PubMed]